

Article

Characterization and Release Kinetics Study of Active Packaging Films Based on Modified Starch and Red Cabbage Anthocyanin Extract

Meng Cheng, Xiaoran Yan, Yingjun Cui, Minjie Han, Yirong Wang, Juan Wang, Rongfei Zhang and Xiangyou Wang * 

School of Agricultural Engineering and Food Science, Shandong University of Technology, Zibo 255000, China; chengmeng0110@163.com (M.C.); xiaoranyan1222@163.com (X.Y.); cyj522819@163.com (Y.C.); hanminjie123@126.com (M.H.); wyrzhk8090@163.com (Y.W.); wangjuan7912@163.com (J.W.); zrf@sdut.edu.cn (R.Z.)

* Correspondence: wxy@sdut.edu.cn; Tel.: +86-0533-2780897

Abstract: Active packaging films were prepared by adding red cabbage anthocyanin extract (RCAE) into acetylated distarch phosphate (ADSP). This paper investigated the influence of the interaction relationship between RCAE and the film matrix on the structure, barrier, antioxidant and release properties of active films. Sixteen principal compounds in RCAE were identified as anthocyanins based on mass spectroscopic analysis. Micromorphological observations indicated that the RCAE distribution uniformity in the films decreased as the RCAE content increased. When the concentration of RCAE was not higher than 20%, the moisture absorption and oxygen permeability of films decreased. The stability of RCAE in the films was enhanced by the electrostatic interaction between RCAE and ADSP with the formation of hydrogen bonds, which facilitated the sustainability of the antioxidant properties of films. The release kinetics of RCAE proved that the release rate of RCAE in active films was the fastest in distilled water, and Fickian's law was appropriate for portraying the release behavior. Moreover, the cytocompatibility assay showed that the test films were biocompatible with a viability of >95% on HepG2 cells. Thus, this study has established the suitability of the films for applications in active and food packaging.

Keywords: active packaging; antioxidant activity; anthocyanin; release kinetics



Citation: Cheng, M.; Yan, X.; Cui, Y.; Han, M.; Wang, Y.; Wang, J.; Zhang, R.; Wang, X. Characterization and Release Kinetics Study of Active Packaging Films Based on Modified Starch and Red Cabbage Anthocyanin Extract. *Polymers* **2022**, *14*, 1214. <https://doi.org/10.3390/polym14061214>

Academic Editor: Sergio Torres-Giner

Received: 21 February 2022

Accepted: 15 March 2022

Published: 17 March 2022

Publisher's Note: MDPI stays neutral with regard to jurisdictional claims in published maps and institutional affiliations.



Copyright: © 2022 by the authors. Licensee MDPI, Basel, Switzerland. This article is an open access article distributed under the terms and conditions of the Creative Commons Attribution (CC BY) license (<https://creativecommons.org/licenses/by/4.0/>).

1. Introduction

In the food supply chain, packaging is an essential aspect to maintain food quality, reduce food waste and ensure food safety [1]. In traditional packaging, products are generally protected “passively” by using the barrier properties of the packaging materials [2,3]. Active packaging technology alters the function of the packaging from “passive” to “active”; that is, by adding antibacterial agents, antioxidants, releasing agents, absorbents and other active materials that control the internal environment of the package to better protect food [4,5]. Considering that oxidation is one of the major issues affecting food quality, the incorporation of antioxidants into packaging materials is promising, as they delay food spoilage [6,7]. With the increasing emphasis on food safety, adding natural antioxidants into packaging materials has become a research hotspot in recent years. Some of these natural antioxidants are plant essential oils [8], coconut shell extract [9], bamboo leaves [10], anthocyanin extract [11], and pine needles extract [12].

In recent years, the development of active packaging containing anthocyanins has become an important research area in the field of food engineering [13]. The results show that anthocyanins have strong antioxidant activity due to the presence of a large number of phenolic groups in their molecular structure [14,15]. Wang et al. [16] investigated the antioxidant activity of raspberry anthocyanin and reported that raspberry anthocyanin

could effectively prevent the formation of 2,2'-Azinobis (3-ethyl-benzothiazoline-6-sulfonic acid) diammonium salt (ABTS) and 1,1-diphenyl-2-picrylhydrazyl (DPPH) free radicals. Due to the presence of the cyanidin 3,5-diglucoside, the majoritarian anthocyanin in red cabbage, this feedstock represents a promising source for obtaining anthocyanins in its concentrated form, which can be used as a natural antioxidant [17]. As the basic structure of red cabbage anthocyanin extract (RCAE) is cationic, they are highly susceptible to attack by reactive oxygen anions and free electrons, making them more unstable and susceptible to degradation [18]. In addition to their own structure, environmental factors, such as pH, temperature, light, metal ions, co-pigments and food additives, can also affect the stability of anthocyanins [19,20]. Therefore, it is of great importance to study and improve the stability of anthocyanins during processing and storage, so as to broaden their application scope.

Solid support is another component of active packaging, which plays an important role in fixing antioxidants, blocking the internal environment of packaging and protecting the packaged product. In recent years, some active films with antioxidant activity were prepared by adding anthocyanins or natural extracts into solid supports. Wang et al. [21] developed an antioxidant film by mixing gelatin with anthocyanins nanocomplexes for protecting olive oil from oxidation. The starch/PVA active film loaded with *Lycium ruthenicum* anthocyanins as packaging material can extend the shelf life of refrigerated fish [22]. Acetylated distarch phosphate (ADSP) is an esterified cross-linked composite-modified cassava starch obtained by acetylation and phosphate reactions of native cassava starch. Equally, ADSP films have good thermal stability and tensile strength. In our previous study, we illuminated that the stability of anthocyanins was enhanced by hydrogen bonding and electrostatic interactions between anthocyanin and ADSP [23]. Thus, this paper studied the effect of red cabbage anthocyanin extract (RCAE) as an antioxidant on the properties of active packaging films. By regulating the concentration of the active ingredient (RCAE) in order to adjust such important parameters as moisture absorption and oxygen permeability, which are crucial in the packaging of food products. The work conducted research on physicochemical properties, including morphology, optical and thermal properties, oxygen permeability, moisture absorption, antioxidant properties of the active films. Moreover, the release behavior of RCAE in ADSP-based active films was simulated in four different packaging environments. To ensure consumers safety, the biocompatibility of the active films containing RCAE was assessed on a human liver cancer cell line (HepG2).

2. Materials and Methods

2.1. Materials

Acetylated distarch phosphate (ADSP) was purchased from Dongguan Dongmei Food Co., Ltd. (Guangdong, China). Anthocyanins were extracted from red cabbage (Shandong, China) based on our previous study [23]. Glycerol, absolute ethanol, thiazolyl blue tetrazolium bromide (MTT) and dimethyl sulfoxide (DMSO) were from Sinopharm Chemical Reagent Co., Ltd. (Shanghai, China), and all were of analytical reagent grade. Dulbecco's modified Eagle's medium (DMEM) was purchased from Gibco (Grand Island, NY, USA). The human liver cancer (HepG2) cell line was obtained from the cell bank of the Institute of Biochemistry and Cell Biology, Chinese Academy of Sciences (Shanghai, China).

2.2. Characterization of Red Cabbage Anthocyanin Extract (RCAE)

The components of RCAE were analyzed by the Agilent 1200 HPLC system (Agilent Technologies, Santa Clara, CA, USA) equipped with a 6460 triple quadrupole mass spectrometer according to the methods of Yong et al. [24] and Liu et al. [25]. The data were acquired by the Q-Exactive system using Xcalibur 4.1 software (Thermo Fisher Scientific, Waltham, MA, USA) and processed by TraceFinder™4.1 clinical software (Thermo Fisher Scientific, Waltham, MA, USA). The quantified data were output into the Excel format.

2.3. Preparation of Active Films

In brief, 4 g of ADSP was dissolved and gelatinized in 100 mL of distilled water containing 1.2 g of glycerol as a plasticizer at 90 °C. When the mixture was cooled to 25 °C, RCAE (131.2 g/L) was added to the above solution to obtain final concentrations of 0, 10%, 20%, 30% and 40% (*w/w*), which were designated as S0, S1, S2, S3 and S4, respectively. Then, the film-forming solutions were poured into a plastic mold of equal dimensions (12 cm × 12 cm) to prepare the films and dried in an oven at 45 °C. The films were conditioned (temperature, 25 °C; relative humidity (RH), 50%) for 2 days before commencement of the test.

2.4. Film Characterization

2.4.1. Microstructural Characteristics

The surface morphology of the film samples was revealed by scanning electron microscopy (SEM; JEOL, Tokyo, Japan). The samples were sputtered with gold before the analysis [26]. The surface of the film (size, 15 μm × 15 μm) was photographed by atomic force microscopy (AFM; Nanoscope V, Bruker, MA, USA) and the 3D images of the film were constructed. The spatial resolution of the microscope was 1 nm in the transverse direction and 0.1 nm in the longitudinal direction, and the scanning speed was 1 Hz. The average roughness (Ra) and root mean square roughness (Rq) of the surface of films was calculated by NanoScope Analysis 1.7 software as previously described [27,28].

2.4.2. Thermogravimetric Analysis

The thermal stability of the films was analyzed by heating films at a rate of 10 °C/min (inert atmosphere: 50 mL/min of N₂). The thermal analyses were performed at temperatures ranging from 26 °C to 600 °C [29].

2.4.3. Color Properties and Opacity

The color of the films was evaluated using a portable colorimeter (CR410, Konica Minolta Sensing, Inc., Sakai Osaka, Japan). A white standard color plate was used as a standard during the color measurement, and lightness (*L**) and chromaticity parameters *a** (red–green) and *b** (yellow–blue) were used to characterize the film color. Total color difference (ΔE) was calculated using the following equation [6]:

$$\Delta E = \sqrt{(L - L^*)^2 + (a - a^*)^2 + (b - b^*)^2}$$

where *L*, *a*, and *b* are the color values of the standard color plate.

The film sample (size, 8 mm × 40 mm) was recorded at 600 nm by the Lambda 35 UV–vis spectrophotometer (PerkinElmer Inc., Waltham, MA, USA). The opacity of each film was determined by the method of Hasheminya et al. [30].

$$Opacity = \frac{A_{600}}{X}$$

where *X* is the film thickness (mm), and *A*₆₀₀ is the absorbance of film at 600 nm.

2.4.4. Oxygen Permeability (OP)

The oxygen permeability (OP) of films was measured by an oxygen permeability test system (CLASSIC 216, Labthink Technology Co., Ltd., Jinan, China). All samples were determined at a temperature of 25 °C and a RH of 75% as previously described [31].

2.4.5. Moisture Absorption

The moisture absorption of the films was determined according to the method of Prachayawarakorn and Kansanthia [32]. The films (size, 25 mm × 25 mm) were desiccated

at 105 °C for 6 h and weighed (W_1). Next, the films were incubated at a RH of $99 \pm 1\%$ for 10 days (W_2). The moisture absorption percentage was calculated as follows:

$$\text{Moisture absorption (\%)} = \frac{W_2 - W_1}{W_1} \times 100\%$$

2.4.6. Antioxidant Activity

The antioxidant activity of films was evaluated by the 1,1-diphenyl-2-picrylhydrazyl (DPPH) free radical scavenging assay [33] using a reagent test kit (Solarbio Science & Technology Co., Ltd., Beijing, China). In brief, 0.05 g of the film sample was weighed and added to 1 mL of extraction solution for determination. The antioxidant activity of films stored at 25 °C for 0 and 7 days was determined.

2.4.7. Release Behavior

A release test of RCAE from the films was performed as previously described [34–36]. S4 samples (size, 6 cm × 6 cm) were placed in the brown bottles containing 20 mL of distilled water, 10%, 50% and 95% ethanol solutions. The samples were gently shaken at 100 rpm (25 °C) under dark conditions. The absorbance of sample solutions was determined by a UV spectrophotometer. The *in vitro* release data were fitted to the release kinetic model to understand the effects of the relationship between RCAE and the ADSP matrix.

2.4.8. Cytotoxicity Assay

The cytotoxicity of ADSP-based films on HepG2 cells was evaluated by the MTT assay [37]. HepG2 cells were inoculated at a density of 1×10^4 cells/mL and cultured in 96-well plates containing DMEM for 24 h. The fresh medium was readded after the old medium had been sucked out. For the experimental group, the film samples (S0–S4; diameter, 8 mm) were placed at the bottom of the hole to directly contact HepG2 cells, while no films were used for the blank control group. After 48 h of treatment, the film samples were removed and washed with PBS for three times. Next, 100 μ L of MTT (final concentration, 0.5 mg/mL) was added to each well, and the plates were incubated for 4 h. The medium containing MTT was aspirated, and 200 μ L of DMSO was added to each well to dissolve the formamide crystals. The absorbance at 570 nm was measured, and the blank control group was used to indicate 100% cell viability group.

2.5. Statistical Analysis

All analyses were run in multiples and the results were expressed as means \pm standard deviation. Analysis of variance (ANOVA) and Duncan's new multiple range test were performed at a significance level of $p < 0.05$ using SPSS 19.0 (IBM, Armonk, NY, USA).

3. Results and Discussion

3.1. Identification and Relative Quantification of RCAE

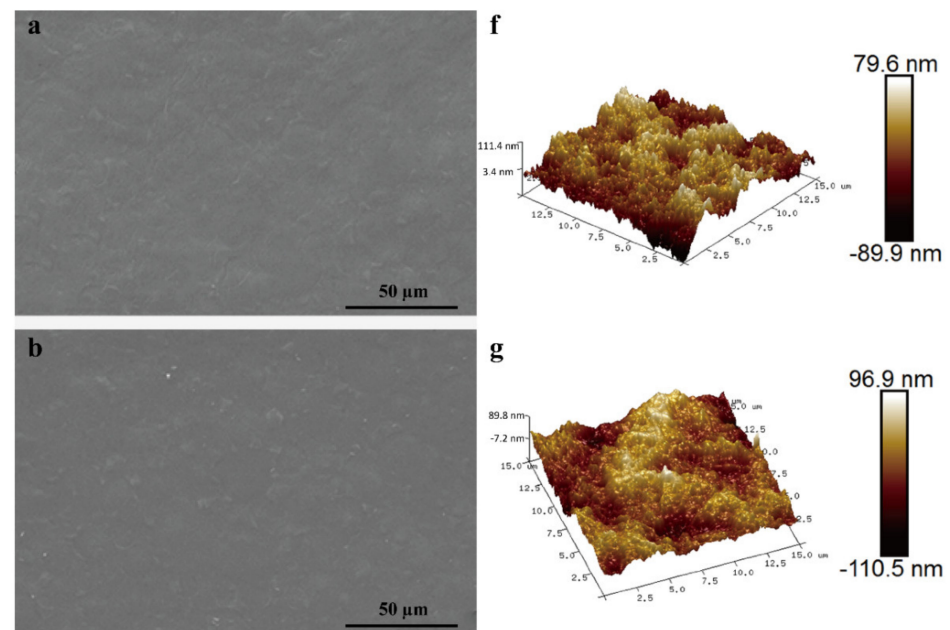
Sixteen anthocyanin structures were identified in RCAE (Table 1). Notably, cyanidin 3,5-diglucoside was characterized as the predominant component, which accounted for 53.913% of the total anthocyanins, followed by delphinidin (31.786%), cyanidin 3-galactoside (5.210%), cyanidin-3-(sinapoyl) (sinapoyl)-diglycoside-5-glycoside (4.611%) and petunidin (2.840%). The other compounds identified in RCAE constituted less than 2% of the total anthocyanins. The components of anthocyanins characterized in this study were somewhat different from those of previous reports [38,39], which could be due to the different varieties, genotypes, cultivation regions and growth conditions of red cabbage. The relative quantification by cyanidin 3,5-diglucoside and the relative content observed for each compound in the LC-MS analysis are illustrated in Table 1. Notably, RCAE contained acylated molecules (cyanidin-3-(sinapoyl) (sinapoyl)-diglycoside-5-glycoside).

Table 1. Characteristics of anthocyanins found in RCAE with their relative amounts.

Compound	Molecular Formula	[M+H] ⁺ (m/z)	Retention Time (min)	Relative Quantification (ng/mL)	Relative Content (%)
Cyanidin 3,5-diglucoside	C ₂₇ H ₃₁ O ₁₆	611.16	2.66	6938.769 ± 23.841	53.913 ± 0.185
Cyanidin 3-galactoside	C ₂₁ H ₂₁ O ₁₁	449.11	3.89	670.568 ± 10.772	5.210 ± 0.084
Cyanidin-3-(sinapoyl)(sinapoyl)-diglucoside-5-glicoside	C ₄₃ H ₆₄ N ₂ O ₃₆	1185	4.24	593.481 ± 11.219	4.611 ± 0.087
Delphinidin	C ₁₅ H ₁₁ O ₇	303.05	4.71	4090.924 ± 16.021	31.786 ± 0.124
Procyanidin B4	C ₃₀ H ₂₆ O ₁₂	579.15	5.35	7.710 ± 0.318	0.060 ± 0.002
Cyanidin	C ₁₅ H ₁₁ O ₆	287.06	5.39	7.444 ± 0.521	0.058 ± 0.004
Procyanidin B2	C ₃₀ H ₂₆ O ₁₂	579.15	5.46	0.720 ± 0.053	0.006 ± 0.004
Petunidin	C ₁₆ H ₁₃ O ₇	317.07	5.57	365.524 ± 5.647	2.840 ± 0.044
Pelargonidin	C ₁₅ H ₁₁ O ₅	271.06	6.02	0.866 ± 0.524	0.007 ± 0.004
Malvidin	C ₁₇ H ₁₅ O ₇	331.08	6.21	4.278 ± 0.306	0.033 ± 0.002
Peonidin	C ₂₂ H ₂₃ O ₁₁	301.07	6.18	67.232 ± 3.499	0.522 ± 0.027
Rutin	C ₂₇ H ₃₀ O ₁₆	611.16	6.78	3.610 ± 0.041	0.028 ± 0.001
Luteolin	C ₁₅ H ₁₀ O ₆	287.06	8.17	37.580 ± 2.314	0.292 ± 0.018
Quercetin	C ₁₅ H ₁₀ O ₇	303.05	8.19	50.118 ± 2.597	0.389 ± 0.020
Isorhamnetin	C ₁₆ H ₁₂ O ₇	317.07	8.36	14.548 ± 1.573	0.113 ± 0.012
Kaempferol	C ₁₅ H ₁₀ O ₆	287.06	8.35	16.808 ± 3.112	0.131 ± 0.024

3.2. Morphology and Structure Analysis

The microstructure of films was investigated by SEM to further explain the relationship between structures of the films and related properties. The surface of S0 films was uniform and smooth (Figure 1a). By contrast, the films incorporated with RCAE showed rougher surfaces (Figure 1b–e), which was indicative of the uneven mixing of ADSP, RCAE and glycerol in the film. The poor distribution of the anthocyanins in the films produced by casting could be related to the convective flow during drying that lifts the particles to the surface and to the poor chemical affinity between anthocyanins and the polymer matrix. Similar observations have been confirmed earlier [40]. Vedove, Maniglia and Tadini [41] also found that the surface of the cassava starch-based films was also roughened by the addition of anthocyanins.

**Figure 1.** Cont.

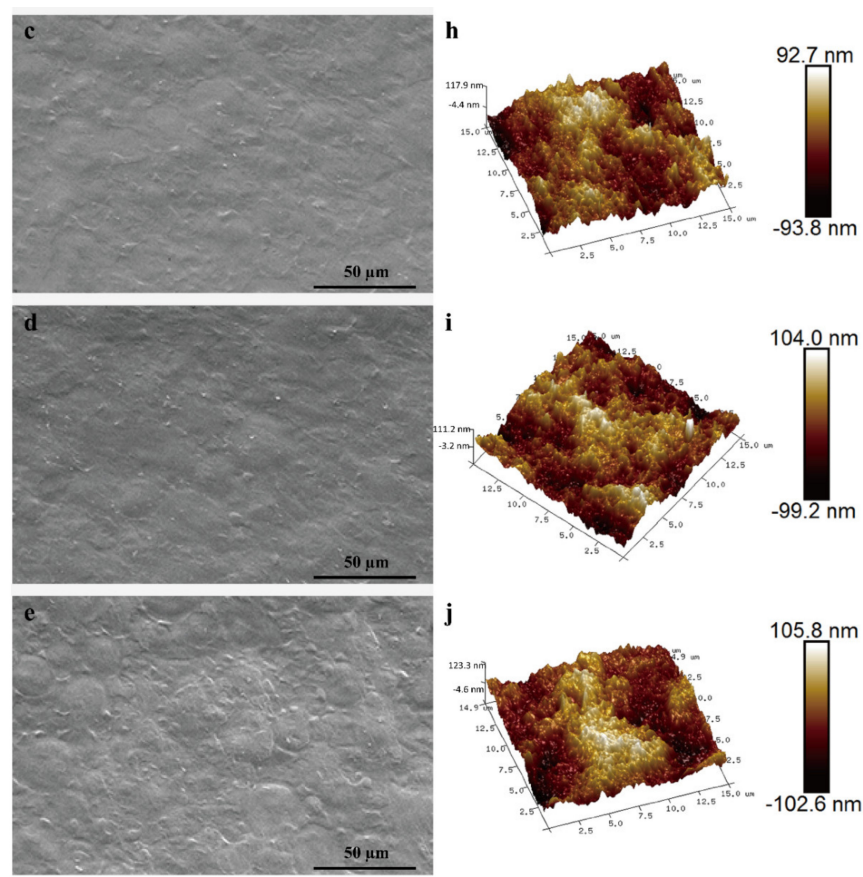


Figure 1. SEM (a–e) and AFM (f–j) images of active films with different RCAE contents: S0 (a,f), S1 (b,g), S2 (c,h), S3(d,i), and S4 (e,j).

The 3D topography of active films was performed by AFM, as shown in Figure 1f–j. The AFM images of S0 films showed revealed a smooth surface with lower Ra and Rq values of 17.7 nm and 22.4 nm, respectively (Table 2). The images of S2 films exhibited a hill-valley structure with Ra and Rq values of 21.0 nm and 26.3 nm, respectively. Similarly, the images of S4 films also depicted an irregular surface with Ra and Rq values of 26.3 nm and 32.3 nm, respectively (Table 2). Adding immiscible filler particles gave higher variation in surface height and roughness of the films. The roughness differences between S0 and S4 films were consistent with the SEM observations. In fact, too much RCAE was incorporated into the ADSP polymer, which was not conducive to the dispersion of the films, resulting in the formation of aggregates in the films. Zhang et al. [42] testified that aggregates appeared on the surface of sodium carboxymethyl starch/ κ -carrageenan films after the addition of the anthocyanin extract. In addition, the surface roughness of gelatin films increased with the incorporation of anthocyanins in the films [21]. Eze et al. [43] also reported similar findings.

Table 2. Roughness parameters, barrier properties, moisture absorption and cell viability of active films with different RCAE contents.

Film Type	Ra (nm)	Rq (nm)	OP ($\times 10^{-14} \text{ cm}^2 \text{ s}^{-1} \text{ Pa}^{-1}$)	Moisture Absorption (%)	Cell Viability (%)
S0	17.7 \pm 0.2 ^a	22.4 \pm 0.4 ^a	2.43 \pm 0.13 ^a	20.36 \pm 0.29 ^a	97.04 \pm 0.31 ^a
S1	18.8 \pm 0.6 ^b	23.5 \pm 0.3 ^b	2.06 \pm 0.18 ^b	18.14 \pm 0.23 ^b	96.38 \pm 0.52 ^{ab}
S2	21.0 \pm 0.8 ^c	26.3 \pm 0.5 ^c	1.71 \pm 0.07 ^c	16.98 \pm 0.31 ^c	95.69 \pm 0.78 ^b
S3	24.0 \pm 0.4 ^d	30.2 \pm 0.2 ^d	1.78 \pm 0.09 ^c	17.05 \pm 0.26 ^c	95.72 \pm 0.15 ^b
S4	26.3 \pm 0.7 ^e	32.3 \pm 0.6 ^e	4.31 \pm 0.20 ^d	23.07 \pm 0.34 ^d	95.59 \pm 0.27 ^b

The values are presented as means \pm SD. Different letters within the same column indicate significant differences ($p < 0.05$).

3.3. Thermal Analysis

The thermal stability of the films was checked by the TGA and DTG curves. The TGA and DTG thermograms of S0, S1, S2, S3 and S4 films are shown in Figure 2. The first stage (30–105 °C) was attributed to the evaporation of loosely bound water in films [44]. The next reduction in mass, which was observed around 105–249 °C, corresponded to the decomposition of glycerol [45]. Finally, the final weight loss between 250–460 °C was related to the polymer degradation in the films [46]. As shown in Figure 2b, the peak of maximum degradation decreased as the RCAE amount increased. This behavior was probably due to the decomposition of volatile molecules present in the RCAE [27]. Prietto et al. [39] found similar results for starch films incorporated with anthocyanins, suggesting less thermal stability of the films. The findings were also reported by Freitas et al. [27], whose cellulose acetate films displayed less thermal stability in the film when incorporated with red cabbage extract. In addition, this result could be related to the interaction weakening in the polymer chains when RCAE was added, which facilitated its decomposition at lower temperatures. As shown in Figure 2b, the S0 films exhibited a peak maximum at 318 °C, whereas the ADSP-RCAE films presented peak maximum at 297–316 °C. The corresponding maximum temperature for the thermal degradation of S4 films was only 21 °C lower than that of S0 films. These results indicated that the active films remain stable at 200 °C, which was suitable for most of the food packaging applications.

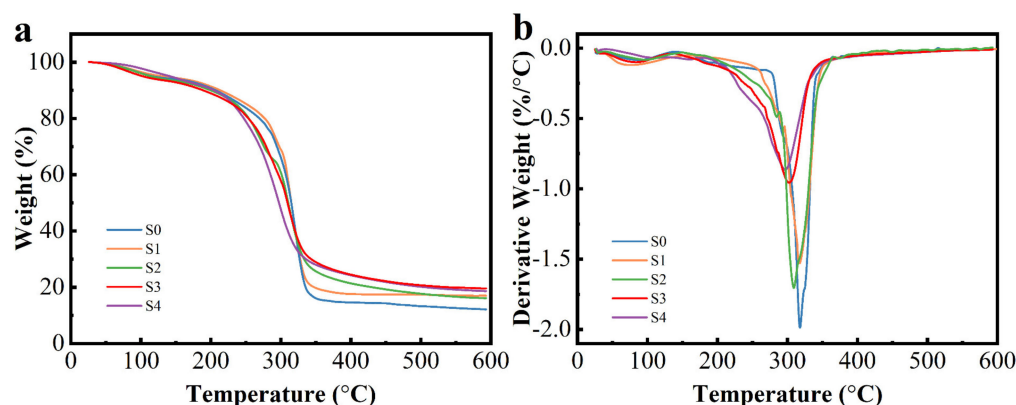


Figure 2. TGA (a) and DTG (b) curves of ADSP-based films added by different RCAE contents.

3.4. Color Properties and Opacity

The packaging films should possess the barrier ability of light to prevent the oxidation of food. The optical properties of films depend on their microstructure, which are affected by the surface and internal heterogeneity of the structure [47]. As demonstrated in Table 3, after incorporating the RCAE in the active films the opacity improved with an enhancement in the RCAE content ($p < 0.05$), indicating that RCAE could increase the opacity of ADSP-based films. These results were in accordance with the color of the active films. After the addition of the RCAE, the values of L^* and b^* reduced, and a^* and ΔE significantly increased ($p < 0.05$). This indicated that the films became redder and had higher opacity. This phenomenon may be caused by the original color of the RCAE. Notably, the covered pattern can be clearly observed in each composite film (Figure S1), indicating that the increase in the opacity of the composite film did not affect the observation of packaged food. In addition, morphological and structural analyses revealed that the surface of the films incorporated with RCAE was rougher, which resulted in the formation of the non-uniform film surface. Incorporated RCAE partially replaced void space in the film matrices where light passed through, giving lower light transmission [48,49]. Additionally, the opacity of the S4 film reached 1.342. Wang et al. [50] also reported that the incorporation of black soybean seed coat extract could greatly reduce the transparency of chitosan films. Bai et al. [51] also proved similar findings.

Table 3. Color and opacity of active films with different RCAE contents.

Film Type	L^*	a^*	b^*	ΔE	Opacity (mm^{-1})
S0	96.15 ± 0.06^a	-1.10 ± 0.02^a	1.88 ± 0.11^a	0.76 ± 0.09^a	0.395 ± 0.010^a
S1	93.67 ± 0.18^b	1.91 ± 0.23^b	-0.09 ± 0.01^b	4.08 ± 0.17^b	0.580 ± 0.010^b
S2	89.50 ± 0.43^c	4.92 ± 0.61^c	-1.72 ± 0.52^c	9.25 ± 0.77^c	0.752 ± 0.004^c
S3	86.52 ± 0.39^d	7.36 ± 0.18^d	-3.42 ± 0.14^d	14.53 ± 1.22^d	0.781 ± 0.007^d
S4	82.74 ± 0.06^e	11.20 ± 0.20^e	-6.68 ± 0.78^e	23.07 ± 3.00^e	1.342 ± 0.009^e

The values are presented as means \pm SD. Different letters within the same column indicate significant differences ($p < 0.05$).

3.5. Oxygen Permeability

As shown in Table 2, the OP value of films decreased along with an increase in RCAE content from 0% to 20% (w/w). The $-OH$ from RCAE and ADSP promoted the formation of intermolecular hydrogen bonds, resulting in highly dense and cohesive films. These findings were consistent with a previous study [23]. Wu et al. [49] demonstrated that the incorporation of black rice bran anthocyanins extract decreased the oxygen barrier properties of the active films. However, the OP value of the S4 films significantly increased to $4.31 \times 10^{-14} \text{ cm}^2 \text{ s}^{-1} \text{ Pa}^{-1}$ ($p < 0.05$). With the gradual increase in RCAE content, the free positive charges prevented the electrostatic attraction between ADSP and anthocyanin. The dense network structure of films was loosened, thus expanding the free volume inside the molecular and facilitating the movement of the molecular chains [27,52]. Moreover, the surface of the films became rougher after the addition of RCAE, which resulted in the non-uniform film surface leading to faster diffusion of gas molecules, which ultimately led to an increased in the oxygen permeability (OP) of the ADSP-based films. Freitas et al. [27] also discovered that the oxygen permeability of cellulose acetate-based films could increase.

3.6. Moisture Absorption

Moisture adsorption mainly reflects the uptake by the film matrix, which is usually used to assess the water resistance of a film [53]. Generally, the lower value of these indexes indicate the better water resistance of the film [54]. The moisture absorption test was performed at a RH of $99 \pm 1\%$ for 10 days, and the data are shown in Table 2. The moisture absorption of S0 films was 20.36%, but as the RCAE increased from 10% to 20%, the moisture absorption of the films significantly decreased from 18.14% to 16.98% ($p < 0.05$), which could be related to the electrostatic interactions and hydrogen bonding between RCAE and ADSP. Chi et al. [55] also reported similar findings, which testified that the moisture absorption of k-carrageenan/hydroxypropyl methylcellulose composite films showed a decreasing trend after the addition of grape skin powder. However, the moisture absorption of S4 films increased to 23.07%, and the increasing proportion of $-OH$ groups at higher concentrations of RCAE was the reason for the increased moisture absorption of S4 films. The absorption of moisture by the film surface was conducive to the release of anthocyanins from ADSP and the formation of $-OH$ groups, which controlled the release rate of RCAE in active films.

3.7. Antioxidant Activity

The antioxidant activity of active films was determined by the DPPH radical scavenging capacity. The antioxidant activity could change the color of the DPPH radical into the yellow diphenylpicrylhydrazine complex. The degree of this reaction mostly depends on the hydrogen donating ability of the antioxidant. As shown in Figure 3, the S0 films showed approximately 2.92% of antioxidant activity. The addition of RCAE could significantly improve the scavenging activity against DPPH of active films, which was mainly ascribed to phenolic compounds in RCAE that showed strong antioxidant capacity [43]. The DPPH radical scavenging capacity of the S4 films (time 0 days) reached $45.21 \pm 2.33\%$. These findings indicate that the addition of RCAE enhanced the antioxidant activity of ADSP films, which was mainly due to the strong hydrogen donating ability of RCAE that reduced

the activity of the radicals or completely eliminated them [9,56]. These findings reveal the potential application of ADSP films containing RCAE in antioxidant packaging, as well as the very promising development in functional packaging. Mushtaq et al. [57] found that films with the addition of pomegranate peel extract retarded the oxidation of fats and proteins in cheese. Other studies demonstrated that an increase in phenolic hydroxyl content is critical for improving antioxidant activity [58]. When the active films were stored for 7 days, the DPPH radical scavenging capacity of films decreased slightly compared with that of films stored for 0 days ($p > 0.05$), indicating that RCAE has good stability in ADSP-based films. Interestingly, this was possibly because of the presence of acylated anthocyanin, which can confer better stability to the molecules [59]. Moreover, this may be the result of the formation of stable complexes of RCAE with ADSP through hydrogen bonding and electrostatic interactions, which improved the stability of RCAE.

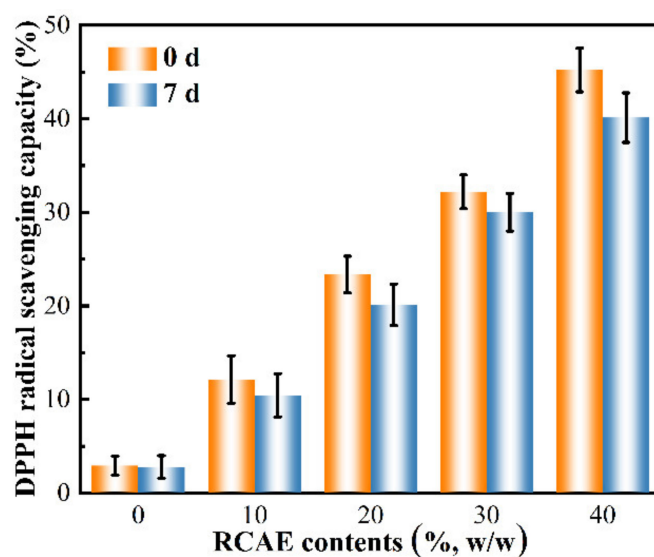


Figure 3. The DPPH radical scavenging capacity of ADSP-based films added by different RCAE contents stored 0 and 7 days placed at 25 °C.

3.8. Release Kinetics

The profiles of kinetic release of RCAE from the ADSP-based active films into simulants in four different packaging environments are presented in Figure 4. The S4 films presented the same behaviour in all simulated solutions, with a burst release in the first 25 h and stabilization afterwards. It is worth noting that the release of RCAE from the films was 0 at the initial moment. When the release time was 169 h, the accumulative release of RCAE from ADSP-based films in distilled water, 10%, 50% and 95% ethanol solutions was 32.08%, 25.79%, 12.48% and 0.23%, respectively. The release of RCAE from the S4 films after 73 h of immersion in distilled water reached equilibrium, showing more than twice as much as in the 50% alcohol solution. These findings revealed that the release rate of RCAE in films was the fastest in distilled water, followed by 10% and 50% alcohol solutions, and RCAE was released slowest in the 95% alcohol solution. In general, the release of active compounds is influenced by the water solubility of the polymer, swelling rate, type of extracted food simulant and diffusion of active compounds from the film to the simulant [60]. The high swelling of films in water and the high solubility of RCAE in water could have promoted in the fast release of RCAE in distilled water. On the contrary, the low solubility of RCAE in alcohol solutions and the insolubility of the ADSP-based films in ethanol solutions could have facilitated the slower release of RCAE from the films in other simulants. Ezati and Rhim [61] reported that the release rate of the films was higher in 50% ethanol solutions than that in water, as well as in 10% and 95% ethanol solutions, and that the release rate of alizarin was solution dependent.

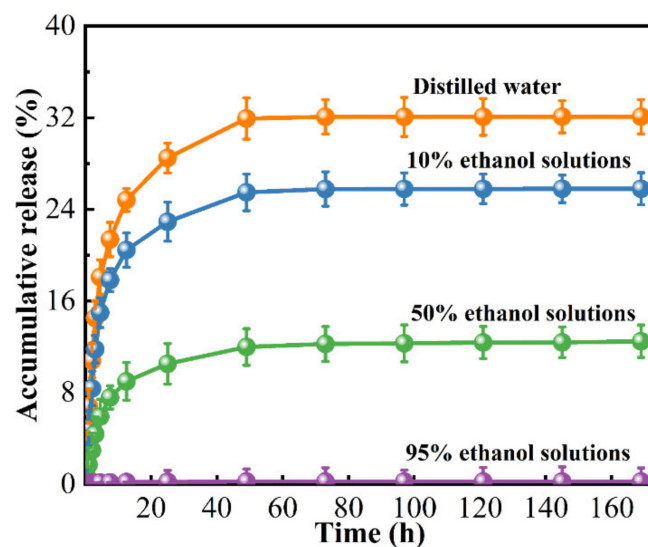


Figure 4. Accumulative release of RCAE from S4 films.

The cumulative release curves can provide valuable information on the release mechanisms and kinetics. The application of the Korsmeyer–Peppas model for the fitness of experimental data pertaining to the release of RCAE from ADSP-based films is shown in Table 4, indicating good predictive power (correlation coefficients (R^2) > 95%). Similarly, Singh et al. [62] demonstrated that the release kinetics of anthocyanin in chitosan/poly(vinyl alcohol) films was best fitted to first-order kinetics from the coefficient of the correlation-fitted data. The results of our investigation showed that Fickian diffusion was suitable for the simulation of RCAE release from ADSP-based films in the four different packaging environments, as evidenced by n values less than 0.5 [63]. Wu et al. [64] reached a similar conclusion. The diffusion property of RCAE from films would be conducive to their sustainable antioxidant activity.

Table 4. Parameters of Korsmeyer–Peppas model at 25 °C for release.

Simulated Solutions	K	n	Correlation Coefficients (R^2)
Distilled water	0.356 ± 0.009	0.332 ± 0.007	0.969 ± 0.001
10% ethanol aqueous	0.303 ± 0.003	0.333 ± 0.010	0.958 ± 0.001
50% ethanol aqueous	0.242 ± 0.002	0.388 ± 0.006	0.963 ± 0.001
95% ethanol aqueous	0.196 ± 0.003	0.426 ± 0.009	0.984 ± 0.003

The values are presented as means ± SD.

3.9. Cytotoxicity Assay

The materials used for food packaging are supposed possess non-toxic characteristics. In the experiment, we found that the cell viability was approximately 95% after 48 h of direct contact between all films and cells ($p > 0.05$). In vitro cytotoxicity studies revealed that these active films were non-cytotoxic packaging materials, in accordance with ISO 10993-5:2009 [65]. Similarly, Andonegi et al. [66] confirmed that chitosan/collagen films were non-cytotoxic biomaterials.

4. Conclusions

In summary, the active films were prepared by the addition of RCAE to ADSP as the film substrate. Morphological and structural analyses showed that the surface of the films became rougher after the addition of RCAE, which caused an uneven film surface. Additionally, the highest average roughness of the S4 films was 26.3 nm. The addition of RCAE improved the light, oxygen barrier properties and water-resistance of films. In addition, these films showed enhanced thermal stabilities and antioxidant activities. These enhancements were attributed to the electrostatic interaction between RCAE and ADSP

with the formation of hydrogen bonds. The release kinetics of RCAE proved that the release rate of RCAE in the films was the fastest in distilled water, and Fickian's law was appropriate for portraying the release behavior. Moreover, these active packaging films also showed great biocompatible capabilities. As such, our findings indicated that the addition of RCAE could improve the physical performance of the ADSP-based films and the composite films had good application potential as packaging films.

Supplementary Materials: The following supporting information can be downloaded at: <https://www.mdpi.com/article/10.3390/polym14061214/s1>, Figure S1: Physical appearances of intelligent packaging films on the white papers.

Author Contributions: Conceptualization, J.W.; data curation, M.C. and M.H.; formal analysis, M.C., Y.C. and R.Z.; funding acquisition, X.W.; investigation, M.C. and X.Y.; methodology, M.C. and Y.W.; project administration, X.W., R.Z. and J.W.; software, M.C. and M.H.; validation, X.Y.; writing—original draft, M.C.; writing—review and editing, J.W. All authors have read and agreed to the published version of the manuscript.

Funding: This work was supported by the National Natural Science Foundation of China (No. 31972144), the Natural Science Foundation of Shandong Province (No. ZR2021MC015, No. ZR2020QC244).

Institutional Review Board Statement: Not applicable.

Informed Consent Statement: Not applicable.

Data Availability Statement: The data presented in this study are available on request from the corresponding author.

Acknowledgments: The authors thank the test support from Shiyanjia Lab (www.shiyanjia.com) (accessed on 14 March 2022).

Conflicts of Interest: The authors declare no conflict of interest.

References

1. Chaudhary, B.U.; Lingayat, S.; Banerjee, A.N.; Kale, R.D. Development of multifunctional food packaging films based on waste Garlic peel extract and Chitosan. *Int. J. Biol. Macromol.* **2021**, *192*, 479–490. [[CrossRef](#)] [[PubMed](#)]
2. Ciannamea, E.M.; Castillo, L.A.; Barbosa, S.E.; De Angelis, M.G. Barrier properties and mechanical strength of bio-renewable, heat-sealable films based on gelatin, glycerol and soybean oil for sustainable food packaging. *React. Funct. Polym.* **2018**, *125*, 29–36. [[CrossRef](#)]
3. Picchio, M.L.; Linck, Y.G.; Monti, G.A.; Gugliotta, L.M.; Minari, R.J.; Alvarez Igarzabal, C.I. Casein films crosslinked by tannic acid for food packaging applications. *Food Hydrocoll.* **2018**, *84*, 424–434. [[CrossRef](#)]
4. Miao, Z.; Zhang, Y.; Lu, P. Novel active starch films incorporating tea polyphenols-loaded porous starch as food packaging materials. *Int. J. Biol. Macromol.* **2021**, *192*, 1123–1133. [[CrossRef](#)]
5. Sooch, B.S.; Mann, M.K. Nanoreinforced biodegradable gelatin based active food packaging film for the enhancement of shelf life of tomatoes (*Solanum lycopersicum* L.). *Food Control* **2021**, *130*, 108322. [[CrossRef](#)]
6. Ma, Y.; Zhao, H.; Ma, Q.; Cheng, D.; Zhang, Y.; Wang, W.; Wang, J.; Sun, J. Development of chitosan/potato peel polyphenols nanoparticles driven extended-release antioxidant films based on potato starch. *Food Packag. Shelf Life* **2022**, *31*, 100793. [[CrossRef](#)]
7. Wang, J.; Sun, X.; Zhang, H.; Dong, M.; Li, L.; Zhangsun, H.; Wang, L. Dual-functional intelligent gelatin based packaging film for maintaining and monitoring the shrimp freshness. *Food Hydrocoll.* **2022**, *124*, 107258. [[CrossRef](#)]
8. Lu, W.; Chen, M.; Cheng, M.; Yan, X.; Zhang, R.; Kong, R.; Wang, J.; Wang, X. Development of antioxidant and antimicrobial bioactive films based on *Oregano* essential oil/mesoporous nano-silica/sodium alginate. *Food Packag. Shelf Life* **2021**, *29*, 100691. [[CrossRef](#)]
9. Tanwar, R.; Gupta, V.; Kumar, P.; Kumar, A.; Singh, S.; Gaikwad, K.K. Development and characterization of PVA-starch incorporated with coconut shell extract and sepiolite clay as an antioxidant film for active food packaging applications. *Int. J. Biol. Macromol.* **2021**, *185*, 451–461. [[CrossRef](#)]
10. Liu, J.; Huang, J.; Hu, Z.; Li, G.; Hu, L.; Chen, X.; Hu, Y. Chitosan-based films with antioxidant of bamboo leaves and ZnO nanoparticles for application in active food packaging. *Int. J. Biol. Macromol.* **2021**, *189*, 363–369. [[CrossRef](#)]
11. Alizadeh Sani, M.; Tavassoli, M.; Salim, S.A.; Azizi-lalabadi, M.; McClements, D.J. Development of green halochromic smart and active packaging materials: TiO₂ nanoparticle- and anthocyanin-loaded gelatin/ κ -carrageenan films. *Food Hydrocoll.* **2022**, *124*, 107324. [[CrossRef](#)]
12. Kadam, A.A.; Singh, S.; Gaikwad, K.K. Chitosan based antioxidant films incorporated with pine needles (*Cedrus deodara*) extract for active food packaging applications. *Food Control* **2021**, *124*, 107877. [[CrossRef](#)]

13. Yong, H.; Liu, J. Recent advances in the preparation, physical and functional properties, and applications of anthocyanins-based active and intelligent packaging films. *Food Packag. Shelf Life* **2020**, *26*, 100550. [[CrossRef](#)]
14. Zhang, X.; Liu, Y.; Yong, H.; Qin, Y.; Liu, J.; Liu, J. Development of multifunctional food packaging films based on chitosan, TiO₂ nanoparticles and anthocyanin-rich black plum peel extract. *Food Hydrocoll.* **2019**, *94*, 80–92. [[CrossRef](#)]
15. Ghareaghajlou, N.; Hallaj-Nezhadi, S.; Ghasempoura, Z. Red cabbage anthocyanins: Stability, extraction, biological activities and applications in food systems. *Food Chem.* **2021**, *365*, 130482. [[CrossRef](#)]
16. Wang, Y.; Ye, Y.; Wang, L.; Yin, W.; Liang, J. Antioxidant activity and subcritical water extraction of anthocyanin from raspberry process optimization by response surface methodology. *Food Biosci.* **2021**, *44*, 101394. [[CrossRef](#)]
17. Machado, M.H.; Almeida, A.D.R.; Maciel, M.V.D.O.B.; Vitorino, V.B.; Bazzo, G.C.; da Rosa, C.G.; Sganzerla, W.G.; Mendes, C.; Barreto, P.L.M. Microencapsulation by spray drying of red cabbage anthocyanin-rich extract for the production of a natural food colorant. *Biocatal. Agric. Biotechnol.* **2022**, *39*, 102287. [[CrossRef](#)]
18. Yao, L.; Xu, J.; Zhang, L.; Zheng, T.; Liu, L.; Zhang, L. Physicochemical stability-increasing effects of anthocyanin via a co-assembly approach with an amphiphilic peptide. *Food Chem.* **2021**, *362*, 130101. [[CrossRef](#)]
19. Martinsen, B.K.; Aaby, K.; Skrede, G. Effect of temperature on stability of anthocyanins, ascorbic acid and color in strawberry and raspberry jams. *Food Chem.* **2020**, *316*, 126297. [[CrossRef](#)]
20. Quan, W.; He, W.; Qie, X.; Chen, Y.; Zeng, M.; Qin, F.; Chen, J.; He, Z. Effects of β -cyclodextrin, whey protein, and soy protein on the thermal and storage stability of anthocyanins obtained from purple-fleshed sweet potatoes. *Food Chem.* **2020**, *320*, 126655. [[CrossRef](#)]
21. Wang, S.; Xia, P.; Wang, S.; Liang, J.; Sun, Y.; Yue, P.; Gao, X. Packaging films formulated with gelatin and anthocyanins nanocomplexes: Physical properties, antioxidant activity and its application for olive oil protection. *Food Hydrocoll.* **2019**, *96*, 617–624. [[CrossRef](#)]
22. Qin, Y.; Yun, D.; Xu, F.; Chen, D.; Kan, J.; Liu, J. Smart packaging films based on starch/polyvinyl alcohol and *Lycium ruthenicum* anthocyanins-loaded nano-complexes: Functionality, stability and application. *Food Hydrocoll.* **2021**, *119*, 106850. [[CrossRef](#)]
23. Cheng, M.; Cui, Y.; Yan, X.; Zhang, R.; Wang, J.; Wang, X. Effect of dual-modified cassava starches on intelligent packaging films containing red cabbage extracts. *Food Hydrocoll.* **2022**, *124*, 107225. [[CrossRef](#)]
24. Yong, H.; Wang, X.; Bai, R.; Miao, Z.; Zhang, X.; Liu, J. Development of antioxidant and intelligent pH-sensing packaging films by incorporating purple-fleshed sweet potato extract into chitosan matrix. *Food Hydrocoll.* **2019**, *90*, 216–224. [[CrossRef](#)]
25. Liu, J.; Yong, H.; Liu, Y.; Qin, Y.; Kan, J.; Liu, J. Preparation and characterization of active and intelligent films based on fish gelatin and haskap berries (*Lonicera caerulea* L.) extract. *Food Packag. Shelf Life* **2019**, *22*, 100417. [[CrossRef](#)]
26. Chen, C.; Zong, L.; Wang, J.; Xie, J. Microfibrillated cellulose reinforced starch/polyvinyl alcohol antimicrobial active films with controlled release behavior of cinnamaldehyde. *Carbohydr. Polym.* **2021**, *272*, 118448. [[CrossRef](#)] [[PubMed](#)]
27. Freitas, P.A.V.; Silva, R.R.A.; de Oliveira, T.V.; Soares, R.R.A.; Junior, N.S.; Moraes, A.R.F.; Pires, A.C.D.S.; Soares, N.F.F. Development and characterization of intelligent cellulose acetate-based films using red cabbage extract for visual detection of volatile bases. *LWT Food Sci. Technol.* **2020**, *132*, 109780. [[CrossRef](#)]
28. Su, C.; Zhang, X.; Ge, X.; Shen, H.; Zhang, Q.; Lu, Y.; Sun, X.; Sun, Z.; Li, W. Structural, physical and degradation characteristics of polyvinyl alcohol/esterified mung bean starch/gliadin ternary composite plastic. *Ind. Crops Prod.* **2022**, *176*, 114365. [[CrossRef](#)]
29. Gürler, N.; Paşa, S.; Temel, H. Silane doped biodegradable starch-PLA bilayer films for food packaging applications: Mechanical, thermal, barrier and biodegradability properties. *J. Taiwan Inst. Chem. Eng.* **2021**, *123*, 261–271. [[CrossRef](#)]
30. Hasheminya, S.; Mokarram, R.R.; Ghanbarzadeh, B.; Hamishekar, H.; Kafil, H.S.; Dehghannya, J. Development and characterization of biocomposite films made from kefiran, carboxymethyl cellulose and *Satureja Khuzestanica* essential oil. *Food Chem.* **2019**, *289*, 443–452. [[CrossRef](#)] [[PubMed](#)]
31. Song, F.; Zhang, B.; Ge, X.; Jiang, Y. Preparation of self-reinforced starch films for use as hard capsule material. *Int. J. Biol. Macromol.* **2021**, *189*, 715–721. [[CrossRef](#)]
32. Prachayawarakorn, J.; Kansanthia, P. Characterization and properties of singly and dually modified hydrogen peroxide oxidized and glutaraldehyde crosslinked biodegradable starch films. *Int. J. Biol. Macromol.* **2022**, *194*, 331–337. [[CrossRef](#)]
33. Cheng, M.; Kong, R.; Zhang, R.; Wang, X.; Wang, J.; Chen, M. Effect of glyoxal concentration on the properties of corn starch/poly(vinyl alcohol)/carvacrol nanoemulsion active films. *Ind. Crops Prod.* **2021**, *171*, 113864. [[CrossRef](#)]
34. Wu, L.T.; Tsai, I.L.; Ho, Y.C.; Hang, Y.H.; Lin, C.; Tsai, M.L.; Mi, F.L. Active and intelligent gellan gum-based packaging films for controlling anthocyanins release and monitoring food freshness. *Carbohydr. Polym.* **2021**, *254*, 117410. [[CrossRef](#)]
35. Liu, J.; Wang, H.; Wang, P.; Guo, M.; Li, L.; Chen, M.; Jiang, S.; Li, X.; Jiang, S. Extract from *Lycium ruthenicum* Murr. Incorporating κ -carrageenan colorimetric film with a wide pH-sensing range for food freshness monitoring. *Food Hydrocoll.* **2019**, *94*, 1–10. [[CrossRef](#)]
36. Bi, F.; Qin, Y.; Chen, D.; Kan, J.; Liu, J. Development of active packaging films based on chitosan and nano-encapsulated luteolin. *Int. J. Biol. Macromol.* **2021**, *182*, 545–553. [[CrossRef](#)]
37. Campoccia, D.; Ravaioli, S.; Santi, S.; Mariani, V.; Santarcangelo, C.; De Filippis, A.; Montanaro, L.; Arciola, C.R.; Daglia, M. Exploring the anticancer effects of standardized extracts of poplar-type propolis: In vitro cytotoxicity toward cancer and normal cell lines. *Biomed. Pharmacother.* **2021**, *141*, 111895. [[CrossRef](#)]
38. Wiczowski, W.; Szawara-Nowak, D.; Topolska, J. Red cabbage anthocyanins: Profile, isolation, identification, and antioxidant activity. *Food Res. Int.* **2013**, *51*, 303–309. [[CrossRef](#)]

39. Prietto, L.; Mirapalhete, T.C.; Pinto, V.Z.; Hoffmann, J.F.; Vanier, N.L.; Lim, L.; Dias, A.R.G.; Zavareze, E.D.R. pH-sensitive films containing anthocyanins extracted from black bean seed coat and red cabbage. *LWT Food Sci. Technol.* **2017**, *80*, 492–500. [[CrossRef](#)]
40. Yuan, B.; Cao, Y.; Tang, Q.; Yuan, Z.; Zhou, Y.; McClemenys, D.J.; Cao, C. Enhanced performance and functionality of active edible films by incorporating tea polyphenols into thin calcium alginate hydrogels. *Food Hydrocoll.* **2019**, *97*, 105197. [[CrossRef](#)]
41. Vedove, T.M.R.D.; Maniglia, B.C.; Tadini, C.C. Production of sustainable smart packaging based on cassava starch and anthocyanin by an extrusion process. *J. Food Eng.* **2021**, *289*, 110274. [[CrossRef](#)]
42. Zhang, C.; Sun, G.; Cao, L.; Wang, L. Accurately intelligent film made from sodium carboxymethyl starch/ κ -carrageenan reinforced by mulberry anthocyanins as an indicator. *Food Hydrocoll.* **2020**, *108*, 106012. [[CrossRef](#)]
43. Eze, F.N.; Jayeoye, T.J.; Singh, S. Fabrication of intelligent pH-sensing films with antioxidant potential for monitoring shrimp freshness via the fortification of chitosan matrix with broken Riceberry phenolic extract. *Food Chem.* **2022**, *366*, 130574. [[CrossRef](#)]
44. Gutiérrez, T.J.; Alvarez, V.A. Bionanocomposite films developed from corn starch and natural and modified nano-clays with or without added blueberry extract. *Food Hydrocoll.* **2018**, *77*, 407–420. [[CrossRef](#)]
45. Koshy, R.R.; Koshy, J.T.; Mary, S.K.; Sadanandan, S.; Jisha, S.; Pothan, L.A. Preparation of pH sensitive film based on starch/carbon nano dots incorporating anthocyanin for monitoring spoilage of pork. *Food Control* **2021**, *126*, 108039. [[CrossRef](#)]
46. Rammak, T.; Boonsuk, P.; Kaewtatip, K. Mechanical and barrier properties of starch blend films enhanced with kaolin for application in food packaging. *Int. J. Biol. Macromol.* **2021**, *192*, 1013–1020. [[CrossRef](#)]
47. Kong, R.; Wang, J.; Cheng, M.; Lu, W.; Chen, M.; Zhang, R.; Wang, X. Development and characterization of corn starch/PVA active films incorporated with carvacrol nanoemulsions. *Int. J. Biol. Macromol.* **2020**, *164*, 1631–1639. [[CrossRef](#)] [[PubMed](#)]
48. Liang, T.; Sun, G.; Cao, L.; Li, J.; Wang, L. A pH and NH_3 sensing intelligent film based on *Artemisia sphaerocephala* Krasch. gum and red cabbage anthocyanins anchored by carboxymethyl cellulose sodium added as a host complex. *Food Hydrocoll.* **2019**, *87*, 858–868. [[CrossRef](#)]
49. Wu, C.; Sun, J.; Zheng, P.; Kang, X.; Chen, M.; Li, Y.; Ge, Y.; Hu, Y.; Pang, J. Preparation of an intelligent film based on chitosan/oxidized chitin nanocrystals incorporating black rice bran anthocyanins for seafood spoilage monitoring. *Carbohydr. Polym.* **2019**, *222*, 115006. [[CrossRef](#)] [[PubMed](#)]
50. Wang, X.; Yong, H.; Gao, L.; Li, L.; Jin, M.; Liu, J. Preparation and characterization of antioxidant and pH-sensitive films based on chitosan and black soybean seed coat extract. *Food Hydrocoll.* **2019**, *89*, 56–66. [[CrossRef](#)]
51. Bai, R.; Zhang, X.; Yong, H.; Wang, X.; Liu, Y.; Liu, J. Development and characterization of antioxidant active packaging and intelligent Al^{3+} -sensing films based on carboxymethyl chitosan and quercetin. *Int. J. Biol. Macromol.* **2019**, *126*, 1074–1084. [[CrossRef](#)]
52. Zhang, C.; Sun, G.; Li, J.; Wang, L. A green strategy for maintaining intelligent response and improving antioxidant properties of κ -carrageenan-based film via cork bark extractive addition. *Food Hydrocoll.* **2021**, *113*, 106470. [[CrossRef](#)]
53. Li, J.; Ye, F.; Lei, L.; Zhao, G. Combined effects of octenylsuccination and oregano essential oil on sweet potato starch films with an emphasis on water resistance. *Int. J. Biol. Macromol.* **2018**, *115*, 547–553. [[CrossRef](#)]
54. Hu, X.; Jia, X.; Zhi, C.; Jin, Z.; Miao, M. Improving properties of normal maize starch films using dual-modification: Combination treatment of debranching and hydroxypropylation. *Int. J. Biol. Macromol.* **2019**, *130*, 197–202. [[CrossRef](#)]
55. Chi, W.; Cao, L.; Sun, G.; Meng, F.; Zhang, C.; Li, J.; Wang, L. Developing a highly pH-sensitive κ -carrageenan-based intelligent film incorporating grape skin powder via a cleaner process. *J. Clean. Prod.* **2020**, *244*, 118862. [[CrossRef](#)]
56. Qin, Y.; Liu, Y.; Yong, H.; Liu, J.; Zhang, X.; Liu, J. Preparation and characterization of active and intelligent packaging films based on cassava starch and anthocyanins from *Lycium ruthenicum* Murr. *Int. J. Biol. Macromol.* **2019**, *134*, 80–90. [[CrossRef](#)]
57. Mushtaq, M.; Gani, A.; Gani, A.; Punoo, H.A.; Masoodi, F.A. Use of pomegranate peel extract incorporated zein film with improved properties for prolonged shelf life of fresh Himalayan cheese (Kalari/kradi). *Innov. Food Sci. Emerg. Technol.* **2018**, *48*, 25–32. [[CrossRef](#)]
58. Zhang, X.; Zhao, Y.; Shi, Q.; Zhang, Y.; Liu, J.; Wu, X.; Fang, Z. Development and characterization of active and pH-sensitive films based on psyllium seed gum incorporated with free and microencapsulated mulberry pomace extracts. *Food Chem.* **2021**, *352*, 129333. [[CrossRef](#)]
59. Zhao, C.L.; Yu, Y.Q.; Chen, Z.J.; Wen, G.S.; Wei, F.G.; Zheng, Q.; Wang, C.D.; Xiao, X.L. Stability-increasing effects of anthocyanin glycosyl acylation. *Food Chem.* **2016**, *214*, 119–128. [[CrossRef](#)]
60. Lee, M.H.; Kim, S.Y.; Park, H.J. Effect of halloysite nanoclay on the physical, mechanical, and antioxidant properties of chitosan films incorporated with clove essential oil. *Food Hydrocoll.* **2018**, *84*, 58–67. [[CrossRef](#)]
61. Ezati, P.; Rhim, J.W. pH-responsive chitosan-based film incorporated with alizarin for intelligent packaging applications. *Food Hydrocoll.* **2020**, *102*, 105629. [[CrossRef](#)]
62. Singh, S.; Nwabor, O.F.; Syukri, D.M.; Voravuthikunchai, S.P. Chitosan-poly(vinyl alcohol) intelligent films fortified with anthocyanins isolated from *Clitoria ternatea* and *Carissa carandas* for monitoring beverage freshness. *Int. J. Biol. Macromol.* **2021**, *182*, 1015–1025. [[CrossRef](#)]
63. Ritger, P.L.; Peppas, N.A. A simple equation for description of solute release I. Fickian and non-fickian release from non-swellable devices in the form of slabs, spheres, cylinders or discs. *J. Control. Release* **1987**, *5*, 23–36. [[CrossRef](#)]
64. Wu, C.; Li, Y.; Sun, J.; Lu, Y.; Tong, C.; Wang, L.; Yan, Z.; Pang, J. Novel konjac glucomannan films with oxidized chitin nanocrystals immobilized red cabbage anthocyanins for intelligent food packaging. *Food Hydrocoll.* **2020**, *98*, 105245. [[CrossRef](#)]

-
65. ISO 10993–5; Biological Evaluation of Medical Devices-Part 5: Tests for In Vitro Cytotoxicity. ISO: Geneva, Switzerland, 2009. Available online: <https://www.iso.org/standard/36406.html>(accessed on 1 February 2022).
 66. Andonegi, M.; Heras, K.L.; Santos-Vizcaíno, E.; Igartua, M.; Hernandez, R.M.; de la Caba, K.; Guerrero, P. Structure-properties relationship of chitosan/collagen films with potential for biomedical applications. *Carbohydr. Polym.* **2020**, *237*, 116159. [[CrossRef](#)]